SANDIA REPORT

SAND2014-17816
Unlimited Release
Printed September 2014

Experimental Confirmation of Water Column Natural Resonance Migration in a BBDB Device

Diana Bull, Budi Gunawan, & Brian Holmes

Prepared by
Sandia National Laboratories
Albuquerque, New Mexico 87185 and Livermore, California 94550

Sandia National Laboratories is a multi-program laboratory managed and operated by Sandia Corporation, a wholly owned subsidiary of Lockheed Martin Corporation, for the U.S. Department of Energy's National Nuclear Security Administration under contract DE-AC04-94AL85000.

Issued by Sandia National Laboratories, operated for the United States Department of Energy by Sandia Corporation.

Available to DOE and DOE contractors from
U.S. Department of Energy
Office of Scientific and Technical Information
P.O. Box 62
Oak Ridge, TN 37831

Telephone: (865) 576-8401
Facsimile: (865) 576-5728
E-Mail: reports@adonis.osti.gov
Online ordering: http://www.osti.gov/bridge

Available to the public from
U.S. Department of Commerce
National Technical Information Service
5285 Port Royal Rd.
Springfield, VA 22161

Telephone: (800) 553-6847
Facsimile: (703) 605-6900
E-Mail: orders@ntis.fedworld.gov
Online order: http://www.ntis.gov/help/ordermethods.asp?loc=7-4-0#online

SAND2014-17816
Unlimited Release
Printed September 2014

Experimental Confirmation of Water Column Natural Resonance Migration in a BBDB Device

Authors: Diana Bull[1], Budi Gunawan[1], & Brian Holmes[2]

[1]Water Power Department
Sandia National Laboratories
P.O. Box 5800
Albuquerque, New Mexico 87185-MS1124

[2]HMRC University of Cork
Ireland

Abstract

Experiments were conducted with a Backward Bent Duct Buoy (BBDB) oscillating water column wave energy conversion device with a scaling factor of 50 at HMRC at University College Cork, Ireland. Results were compared to numerical performance models. This work experimentally verified the migration of the natural resonance location of the water column due to hydrodynamic coupling for a floating non-axisymmetric device without a power conversion chain PCC present. In addition, the experimental results verified the performance model with a PCC of the same non-axisymmetric device when both floating and grounded.

ACKNOWLEDGMENTS

The staff at HMRC (especially Brian Holmes and Brendan Cahill) were instrumental in completing these experiments. This work was funded by the Department of Energies' Wind and Water Power Technologies Office. Sandia National Laboratories is a multi-program laboratory managed and operated by Sandia Corporation, a wholly owned subsidiary of Lockheed Martin Corporation, for the U.S. Department of Energy's National Nuclear Security Administration under contract DE-AC04-94AL85000. SAND Number: 2014-0176 A

CONTENTS

FIGURES

NOMENCLATURE

BBDB	backward bent duct buoy
BEM	boundary element method
DOE	Department of Energy
FSE	free surface elevation
OWC	oscillating water column
PCC	power conversion chain
RAO	response amplitude operator
SNL	Sandia National Laboratories

1. INTRODUCTION

An oscillating water column (OWC) wave energy converter is a structure with an opening to the ocean below the free surface, i.e. a structure with a moonpool. The area above the moonpool is enclosed to create an air chamber which is open to atmosphere through a turbine. The turbine, with its associated control strategy, 'links' the pressure fluctuations in the air chamber to the power produced by the device. A floating OWC requires that both the wave activated structure and the internal free surface elevation be modeled in a hydrodynamically coupled fashion since each absorbs power from the waves. It is the relative motion between the device and the internal free surface that produces pressure fluctuations. Thus, a floating OWC tuned to operate optimally for the given monochromatic environment requires a numerical model incorporating both hydrodynamic coupling as well as PCC linking.

A non-axisymmetric terminator design, the Backward Bent Duct Buoy (BBDB) [1], is modeled in this paper see Figure 1. This device is L-shaped with the opening to the ocean downstream from the wave propagation direction. By hydrodynamically coupling the structural resonant modes with the internal free surface, the location of the internal free surface resonant mode can migrate significantly depending upon the structural resonant modes. Linking the oscillating structure to the internal free surface with a power conversion chain (turbine, generator, storage, and power electronics) makes possible increases in energy conversion at non-resonant locations. [2]

This paper experimentally confirms of the migration of the natural resonance of the water column that occurs due to hydrodynamic coupling in a floating OWC. Experimental confirmation first verifies the natural resonance of the water column for a grounded BBDB. The natural resonance location of the water column for same BBDB is then verified when it is floating without a PCC. Finally, the experimental response of the floating BBDB with a PCC is presented against the numerical predictions.

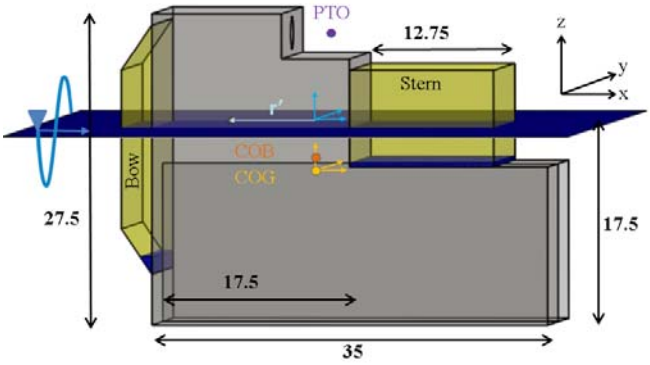

Figure 1. Model of the full-scale BBDB describing dimensions, locations of principal components, locations of the COB and COG, and identifying coordinate systems.

2. FREQUENCY DOMAIN PERFORMANCE MODEL

2.1 Hydrodynamic Formalism

The formalism for a floating OWC followed in this paper is first presented in [2], and it is summarized here for clarity. Two coupled hydrodynamic equations relating to the total force acting on the body and the total volume flow resulting from air-pressure fluctuations govern the dynamics of the device. The total hydrodynamic force, F_{TH}, acting on the j^{th} mode of the body is given by the combination of the excitation force f_j found by holding the body fixed in that direction ($u_j = 0$), the radiated force $\Sigma_{j'} Z_{jj'} u_{j'}$ found by unit-oscillation velocity $u_{j'}$ of the body with the air chamber vented to atmosphere ($p = 0$), and a coupling force H_j^p that accounts for unit-fluctuation of the air-pressure inducing body oscillations:

$$F_{TH,j} = f_j A - \sum_{j'} Z_{jj'} u_{j'} - H_j^p \, p \qquad j = 1, \dots, 6. \qquad 1$$

In Eq. 1, A is the incident wave amplitude at the global origin and $Z_{jj'}$ is the radiation impedance of the j^{th} mode due to unit-oscillation in one of the six j' rigid body modes. The total hydrodynamic volume flow, Q_{TH}, resulting from air-pressure fluctuations is given by the excitation volume flow q found by venting the air-chamber to atmosphere ($p = 0$), the radiated volume flow Yp found by unit-fluctuation of the pressure p in the air-chamber without allowing the body to oscillate ($u_j = 0$), and a coupling force that accounts for unit-oscillation velocities inducing hydrodynamic volume flow:

$$Q_{TH} = qA - Yp - \sum_{j} H_j^u u_{j.} \qquad 2$$

Above Y is the free surface radiation admittance; it is analogous to the radiation impedance of the oscillating structure.

The frequency and directionally dependent hydrodynamic terms in Eq. 1 relating to the floating body are given as standard output from WAMIT v6.4 [3], the BEM solver used in this research. As is discussed more fully in [2], an array of field points defining the interior free surface allows for hydrodynamic parameters relating to the fluctuating air-pressure within the OWC to be calculated using reciprocity relations. [2], [4], [5]

2.1.1 Unlinked & Hydrodynamically Coupled Formalism

When considering an unlinked device with no PCC, there can be no pressure fluctuation in the air chamber since the pressure is vented to atmosphere. Hence in Eq.'s 1 and 2 above, when considering the influence of the coupling term on the unlinked but hydrodynamically coupled device, $p = 0$ should be substituted in. Thus the unlinked hydrodynamically coupled natural resonances for the structure are the peaks associated with phase changes in the total hydrodynamic force given by:

$$F_{TH,j} = f_j A - \sum_{j'} Z_{jj'} u_{j'} \qquad j = 1, \ldots, 6. \qquad 3$$

It is clear from Eq. 3 that the natural resonances for the unlinked device are the same as a hydrodynamically uncoupled device. The unlinked hydrodynamically coupled natural resonance for the oscillating water column is the peak associated with phase change in the total hydrodynamic volume flow given by:

$$Q_{TH} = qA - \sum_{j} H_j^u u_{j.} \qquad 4$$

Eq. 4, however, clearly shows that the coupling term H_j^u will affect the location of the unlinked hydrodynamically coupled oscillating water column natural resonance. The magnitude of the coupling in comparison to the magnitude of the other term will determine the influence of the coupling on the resonance location.

2.1.2 Unlinked & Hydrodynamically Uncoupled Formalism

When considering the case of a grounded OWC, the body no longer reacts freely to the incident waves and hence Eq. 1 is no longer necessary to describe the dynamics of the body. Additionally, there is no longer a coupling term in Eq. 2. Further, if the system is unlinked there will be no pressure fluctuation and thus $p = 0$. Hence the natural resonance location of an unlinked, uncoupled OWC is the peak associated with the phase change in the following relationship:

$$Q_{TH} = qA. \qquad 5$$

2.2 Performance Model

Once the device is linked with a PCC, the device dynamics are expected to change due to the inclusion of the dynamics of the PCC. A Wells Turbine, which possesses a linear relationship between pressure and flow, is assumed in this performance model. The slope between pressure and flow, R_{load}, can be altered *in situ* by adjusting the rate at which the turbine spins. The total power absorbed by the coupled and linked device is dependent upon the R_{load} applied at the air turbine. Air compressibility is modeled assuming a linearized isentropic relationship. Hence with these representations the total hydrodynamic volume flow in the linked system is given by:

$$Q_{TH} = \left(\frac{1}{R_{load}} + i\frac{\omega \forall_\circ}{\gamma P_{atm}}\right) p. \qquad 6$$

The linearized air compressibility is defined through the following terms: the initial volume is $\forall_\circ, \gamma = 1.4$, and is the ratio between the constant-pressure and constant-volume specific heats for air, and p_{atm} is the atmospheric pressure. Additionally, constant viscous damping terms are

applied across all frequencies and added to the right hand sides of Eq.'s 1 and 2 as losses ($-b_{vis,j}u_j$ and $-\frac{1}{R_{vis}}p$ respectively).

3. EXPERIMENTAL CONDITIONS

The device described in [2] was tested using Froude scaling with a scaling factor of 50. A relatively linear representational power conversion chain was constructed by selecting combinations of damping layers and altering the area of an opening (91 mm width, variable length from 0 mm to 380 mm) through which the air fluctuations could pass. The damping layers were composed of felt material of differing thickness and porosity. This method and the materials have been adopted from work at Instituto Superior Técnico in Lisbon Portugal. This representation allowed for a specified scaled $R_{load}$to link the free surface and structure. Each combination of damping layers were calibrated over appropriate pressure ranges in a separate experimental apparatus to determine the most accurate relationship between pressure and flow, i.e. the value of R_{load}.

The experiments were conducted at HMRC at University College Cork in Ireland. Testing of the hydrodynamically uncoupled device was performed in the flume (26 m in length, 3 m in width, and 1.0 m in water depth). A period sweep of regular small amplitude waves were run at the scaled device. The device was situated in a forward facing manner and was placed on cement blocks to obtain a reasonable draft. The regular waves were not pre-calibrated. One *in situ* capacitive wave probe (located in front of the device) provided the wave height measurement for each regular wave and the basis for the response amplitude operator (RAO) calculation.

Testing of the hydrodynamically coupled device was performed in the basin (28 m in length, 18 m in width, and 1.0 m in water depth). Again, period sweeps of regular small amplitude waves were run at the device. The device was situated in a backward facing manner, secured with two mooring lines, and ballasted to obtain the desired draft. All waves were pre-calibrated and this wave height was used in the RAO calculation. Figure 2 shows the layout of the device in the basin.

The device motions and the internal free surface elevation (FSE) were tracked in three dimensions with a Qualisys system. In the flume only the starboard side of free surface was measured while in the basin both the port and starboard sides were measured. A pressure sensor recorded the pressure inside of the air chamber. A load sensor recorded the starboard mooring line tension.

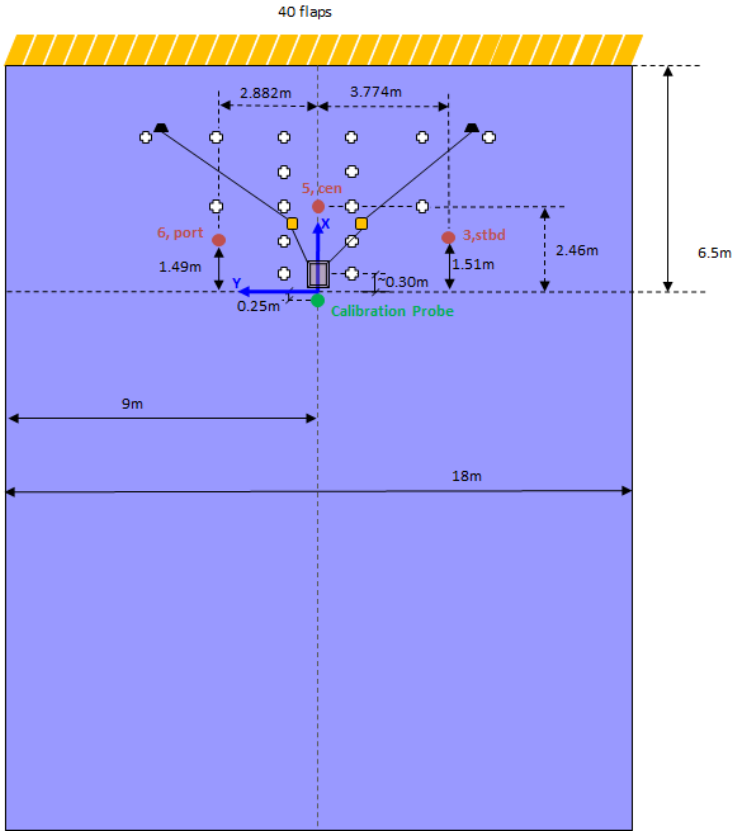

Figure 2. Diagram of the experimental set-up in the HMRC Basin. The BBDB device is indicated with a square and the mooring lines are reproduced as closely as possible. The white crosses are painted on the floor of the basin. The red circles are the wave sensors that were in place during the experiments. The green sensor indicates the location of the wave probe that was used during calibrations and as the basis for RAO calculation.

4. RESULTS

Experimentally derived RAOs are compared to numerical predictions for the same incident waves. Results are shown in full scale. Although the experimental data is capable of calibrating the selected viscous damping values, this is not implemented. For the presented performance model predictions $b_{vis} = 0.02(2\sqrt{M_{tot}c_{tot}})$ and $R_{vis}^{-1} = 0.01(\max(G))$. M_{tot} is the physical mass in combination with the infinite frequency added mass and c_{tot} is the total restoring force. Experimentation at this scale renders air compressibility irrelevant; however, the effects of air compressibility are accounted for in the numerical model as detailed in Eq. 6.

Figure 3 shows the results for a hydrodynamically uncoupled, linked BBDB (i.e. grounded with a PCC). An experimental resistive load of 25 Pa/m^3/sec was applied to the system. Since the dynamics of the structure do not influence the water column, the largest response is located at the expected 'piston' resonance location as illustrated in the subfigures. The experimental FSE and volume flow RAOs match the model prediction magnitude and shape. The volume flow RAO was derived from both the starboard FSE measurements (triangles) as well as the calibration data (circles). When the calibration data is used, the pressure measurement is divided by the calibrated to obtain the volume flow.

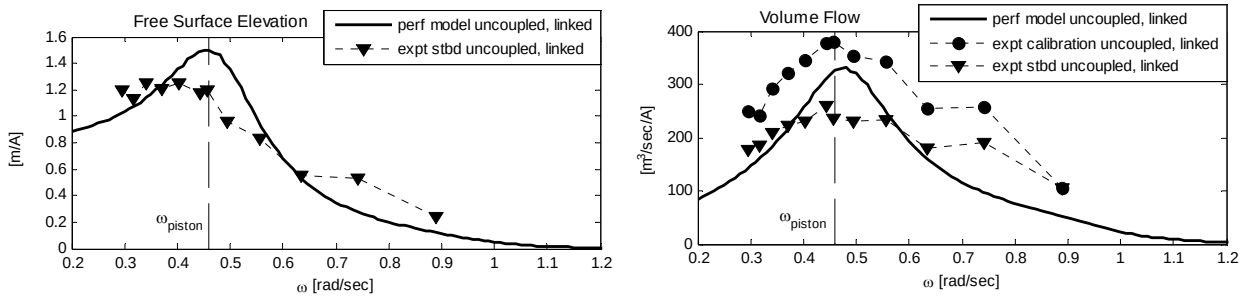

Figure 3. Comparison of the full scale FSE and volume flow RAOs for a hydrodynamically uncoupled but linked device. An experimentally applied R_{load}=25 Pa/m^3/sec was implemented in the performance model. ω_{piston}=0.46 *rad/sec*.

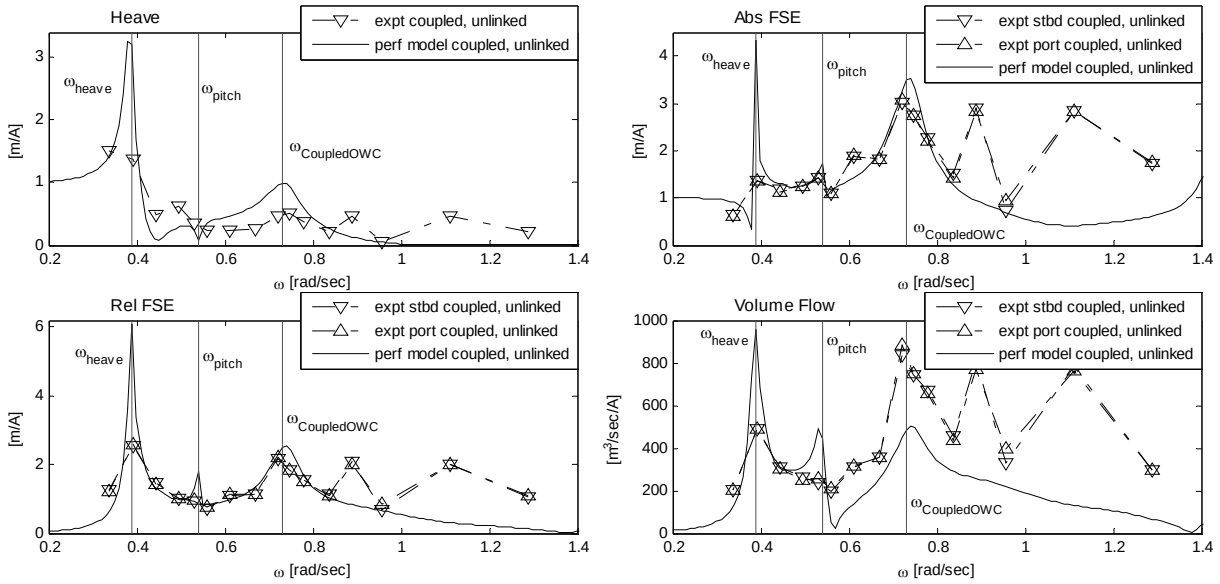

Figure 4. Comparison of the full scale heave, FSE's (absolute and relative), and volume flow RAOs for a hydrodynamically coupled, unlinked BBDB. $\boldsymbol{\omega_{heave} = 0.39\ rad/sec}$, $\boldsymbol{\omega_{pitch} = 0.54\ rad/sec}$, and $\boldsymbol{\omega_{CoupledOWC} = 0.73\ rad/sec}$.

Figure 4 shows selected results for a hydrodynamically coupled, unlinked BBDB. In this case, the dynamics of the structure do influence the water column, as given in Eq. 4, and thus the water column resonance has migrated to a new location. The new resonance location is identified in the subfigures as well as the structural resonance locations. The FSE plots (both absolute and relative to the structure) confirm the predicted hydrodynamically coupled OWC resonance location by exhibiting a large response. Further, the heave and volume flow experimental RAOs confirm the predicted shapes.

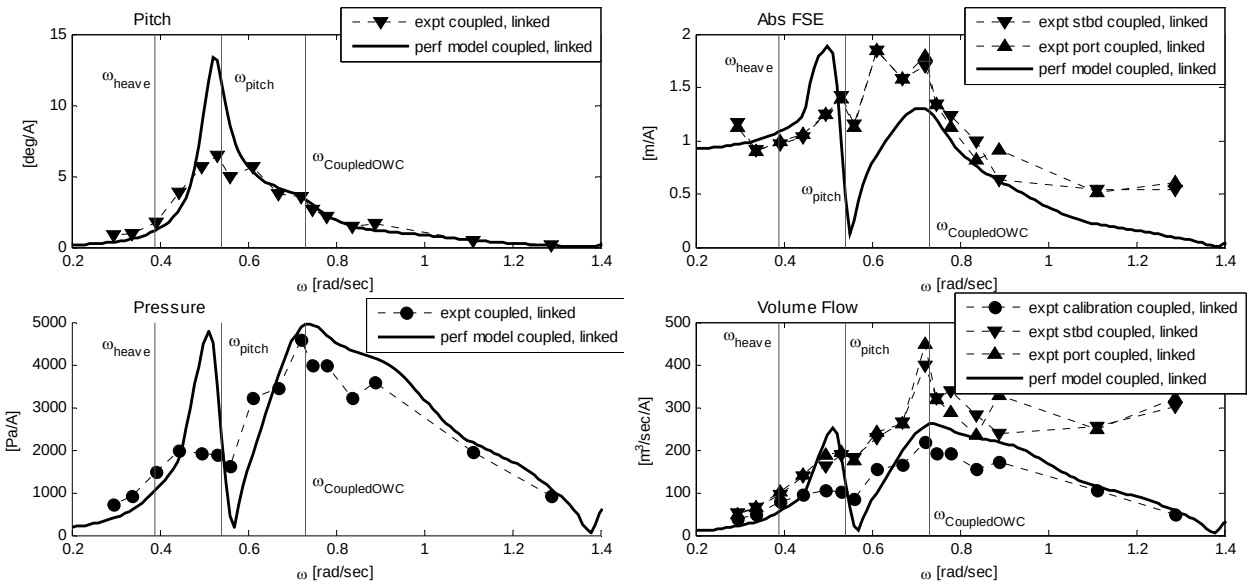

Figure 5. Comparison of the full scale pitch, absolute FSE, pressure, and volume flow RAOs for a hydrodynamically coupled and linked BBDB. An experimentally applied R_{load}=19 Pa/m^3/sec was implemented in the performance model.

Figure 5 shows selected results for a hydrodynamically coupled, linked BBDB. The expected resonance locations are identified on the subfigures. An experimental resistive load of 19 Pa/m3/sec was applied to the system. Again, comparison of experimental to predicted results confirm the peaks, shoulders, and valleys.

At large radial frequencies, the predicted and experimentally determined values begin to diverge in all of the comparisons. However, the statistics reveal a large standard deviation resulting in a large error. Further, due to internal sloshing and higher order modes the measured FSE presents unreliable measurements in some cases. Thus the volume flow is always calculated using multiple methods.

5. REFERENCES

[1] Y. Masuda, T. Yamazaki, Y. Outa, and M. McCormick, "Study of Backward Bent Duct Buoy," in *OCEANS '87*, 1987, pp. 384–389.

[2] D. Bull and E. Johnson, "*Optimal Resistive Control Strategy for a Floating OWC Device*," SAND2013-6198C.

[3] *WAMIT v6.4*. Chestnut Hill, Massachusetts: WAMIT, Inc.

[4] J. Falnes, *Ocean Waves and Oscillating Systems: Linear Interactions Including Wave-Energy Extraction*. Cambridge University Press, 2002.

[5] C. H. Lee and F. G. Nielsen, "*Analysis of oscillating-water column device using a panel method,*" presented at the 11th International Workshop on Water Waves and Floating Bodies, Hamburg Germany, 1996.

DISTRIBUTION

1	HMRC University of Cork Attn: Brian Holmes Youngline Industrial Estate Pouladuff Road Cork, Ireland Email: hmrc@ucc.ie		(electronic copy)
1	MS0734	Margaret Gordon	6124 (electronic copy)
1	MS1124	Diana Bull	6122 (electronic copy)
1	MS1124	Budi Gunawan	6122 (electronic copy)
1	MS0899	Technical Library	9536 (electronic copy)


Sandia National Laboratories